J Mater Sci (2007) 42:4087–4097
DOI 10.1007/s10853-006-1114-4

Anodic oxidation of tantalum in water and biological solutions using current limiting constant voltage method

Sylvanus N. Wosu

Received: 26 January 2005 / Accepted: 15 December 2005 / Published online: 3 May 2007

Abstract A reliable method is developed for preparing tantalum pentoxide film targets in natural water and biological fluids (urine, blood plasma and serum) by the anodization of tantalum metal using a current limiting constant voltage method. Tantalum pentoxide film targets are successfully prepared at a current density of 10 mA cm^{-2} at an anodic voltage ranging from 20 V to 100 V without any oxide breakdown. The results show that for the same applied voltage, more ionic concentration in biological solutions leads to a higher rate of oxide growth than in water and a darker interference color. The analysis shows that anodic oxidation is more likely to breakdown in a biological environment than in pure water for the same oxidation time and applied voltage. The oxide film capacitance is found to be only slightly dependent on pH and anodic voltage with higher capacitive films in biological solutions than for water.

Introduction

Tantalum pentoxide has been extensively studied in the last decade because of its wide applications in the semiconductor industries [1] and medical sciences [2, 3]. Common methods of deposition include anodic or thermal oxidation [4, 5], vacuum evaporation [6], sputtering [7] atomic layer epitaxy [8, 9], and chemical vapor deposition [10]. Oxidization of Ta in some common electrolytes including ammonium citrate water solutions has received considerable attention by several authors [11, 12]. The thickness of the anodic oxide films depends on the type of metal substrate, experimental conditions, pH and nature of the electrolyte, the current efficiency, and the potential difference across it [13, 14]. Certain physical properties of the film and the anodic oxide breakdown tendencies may also be influenced by the composition of the electrolyte [15, 16]. Studies on the influence of electrolyte ion incorporation on the quality of the film, transport process and mechanism of anodic oxide breakdown show that the voltage at which an oxide breaks down depends on the composition [17–19], the conductivity of the electrolyte [20], and the anodized metal [21]. Tantalum anodic films formed in concentrated H_3PO_4 and H_2SO_4 at room temperature have been reported to increase incorporation of electrolyte species into the film. The outer layer of an oxide film grows by metal ion motion and may take up anions from the electrolyte while the inner layer grows by oxygen transport [22, 23]. Badawy et al. [24] investigated the effects of formation voltage, formation current density and passivation medium on the properties and stabilities of the tantalum oxide films and showed that tantalum films could be stable under different aggressive environments. It was shown that the stability of the passive film depends upon the ambient electrolyte.

Anodic oxidation is commonly done at a constant current density. A theoretical description of the dependence of oxide thickness on electric field strength at constant voltage stage has been established by Albella and others [25].

The motivation for the work presented in this paper is the development of a possible oxygen sensor for medical applications. The objective of the work was then to develop a reliable method of preparing Ta_20_5 in natural and ^{18}O-enriched water and biological fluids (urine, blood

S. N. Wosu (✉)
Department of Mechanical Engineering,
University of Pittsburgh, Pittsburgh, PA 15261, USA
e-mail: eodadmin@engr.pitt.edu

plasma and serum) by the anodization of tantalum metal using a current limiting constant voltage method. The $Ta_2{}^{18}O_5$ targets prepared in such solutions in their natural buffered state without any other pre-treatment have been applied in the measurement of $H_2^{18}O$ dilution space and total body water using $^{18}O(p, \alpha)^{15}N$ nuclear reaction analysis of the oxide film targets [2, 3]. The paper also describes the electrochemical cell used in the anodic process.

Biological solutions have a near neutral pH, ranging from 6.5 to 8 such that H^+ concentration is small compared to the OH^- ion from the water. In such neutral solutions, the growth of oxide is expected to occur with equal contribution from metal ion and oxygen ion movement. The balanced half-cell reactions at the electrodes and corresponding net reaction are given as:

$$\begin{aligned} \text{Anode}: \quad & Ta = Ta^{5+} + 5e^- \\ \text{Cathode}: \quad & 2H_2O + 2e^- = 2OH^- + H_2 \\ \text{Net}: \quad & 2Ta + 5H_2O = Ta_2O_5 + 5H_2 \end{aligned} \tag{1}$$

The equation gives a net cell reaction for anodic oxidation of tantalum in water involving the reaction of Ta^{5+} ions with O^- ions in solution to form tantalum pentoxide film with a charge number, $z = 10$. For a well-prepared metal surface and no break down, the process involves no oxygen evolution at the anode although hydrogen gas has been observed to evolve at the cathode.

An ideal supporting electrolyte serves the important function of carrying the current through the solution without incorporating its ions or exchangeable oxygen into the oxide film. For measurements of ^{18}O concentration of the order of natural abundance using nuclear reaction analysis, it is important that the exchange of oxygen ions be minimized as much as possible because any such isotopic exchange outside the dilution process may give incorrect results. Thus, the conventional method of adjusting the pH level by dissolving an appropriate weight fraction of a salt in the aqueous solution of interest is not acceptable for this application. Different concentrations of salt in solution give different results, poor reproducibility, and different oxide breakdown characteristics. A preliminary investigation of oxygen-free salts such as potassium iodide (KI), at 100 V and a current density of 10 mA cm^{-1} resulted in the precipitated iodine ions contaminating the electrolyte, making the solution unsuitable for further use.

The first specific objective was to develop a method that could produce a reproducible, homogeneous oxide film consistently in several biological samples in their untreated, sampled state to preserve the original characteristics of the electrolyte for biomedical applications. For isotopically enriched solutions, this will reduce errors from possible isotopic exchange and thereby optimize the accuracy of determining the ^{18}O concentration in the samples or using the oxide film as a sensor of oxygen utilization.

The oxide film formed can be characterized in terms of the anodic constant, Å volts $^{-1}$, defined as the reciprocal of the field strength for the formation of the oxides and characterizes the oxide film, the metal substrate and the electrolytic condition [26–28]. The Å volts^{-1} value is used to determine the thickness of the oxide film from the applied anodic voltage.

Experimental

Sample preparation and sample holder

The anode substrate plate is a 0.025 mm thick tantalum metal foil of 99.95% purity. The plates samples were cut in 36.5 × 11.5 mm required sizes to make sure no contamination or contact with touch the surface. The sample was used immediately as obtained from the company after it was de-greased with acetone, rinsed with water and dried. This procedure gave reproducible oxide film growth 95% of the time compared to 90% when chemical polishing procedure was used. The chemical polishing procedure involving varying ratios of mixtures of polishing agents is assumed to eliminate possible oxide film on the tantalum metal deposited by natural process. However, the complexity of the polishing procedure and the possibility of contamination are serious disadvantages that outweigh the advantages.

The sample holder consists of two Lucite frames. One frame is 25 × 12.5 mm with a 10 mm hole equal to the required window size of the oxide film. The produced oxide film takes the shape of the exposed window in the electrolyte as shown in Fig. 1. To mount the sample on the holder, the two frames are masked on one side with a vacuum seal compound. The sample is then sandwiched between the masked sides of frames such that only the tantalum in the window is exposed for conduction and anodization. Any other exposed sides going inside the electrolyte are carefully covered with nail polish and allowed to dry. Any bubbles introduced when lowering the connector to the electrolyte is eliminated as they affect the uniformity of the film.

Anodization apparatus and procedure

The electrochemical cell and experimental setup for the anodic oxidation are also shown in Fig. 1. The electrochemical cell is a cylindrical double compartment cell made of Pyrex glass.

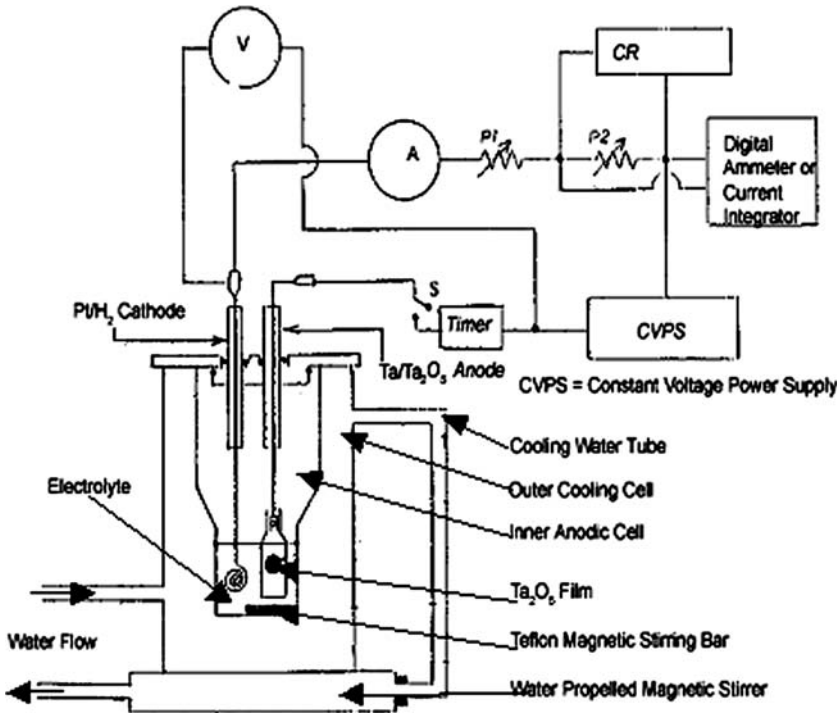

Fig. 1 Electrochemical cell and experimental set up for anodic oxidation showing anodized oxide film in holder

The larger outer compartment houses the inner anodic cell in which the anodic process takes place. Continuous stirring of the electrolyte is accomplished by a Teflon coated micro magnetic stirring bar and a water propelled magnetic stirrer. The cell assembly is placed on the magnetic stirrer such that the water flowing between the cell compartments exits through the magnetic stirrer. The water is pumped and circulated through the system by a partially submersible water pump placed in a water bath and maintained at room temperature of 22 ± 1 °C. The stirring is very important when working with biological solutions. It helps to evenly distribute the ions through the solution in order to eliminate polarization of the electrolyte, thereby maintaining uniform current flow, and uniform solution temperature.

The tantalum substrate serving as the target to be oxidized is part of the anode. The anode assembly is made up of a 0.25 mm diameter platinum wire screwed to an aluminum electrical connector connected the exposed end of tantalum as shown in Fig. 1. The cathode is a platinum electrode arranged helicoidally such that its surface area is equal to the desired surface area of the tantalum oxide film at the anode. It is placed parallel to and in front of the anode so that the current flows uniformly and toward the entire target area.

Current limiting constant voltage anodization

The anode and cathode electrodes are connected to a current-limiting constant voltage power supply. Two current control potentiometers are used to limit the initial anodization current density to a desired value for pre-determined maximum voltage. The power supplymaintains this constant applied voltage and current throughout the duration of the anodic process. However, the potential difference (voltage rise) across the anode increases from zero to this maximum value while the current flowing through the anode drops from the initial maximum value to zero once the timer or switch is on. The initial anodization electric current density (typically 10 mA cm^{-2}) current flowing through the cell is set by potentiometer 1 (P1). The potentiometer 2 (P2) scales the anodic current density as a voltage drop across it. When set at 1 KΩ ohms, a 10 mA is seen by the chart record as 10 V. The total electric current density flowing through the electrolyte at any instant of time is given as:

$$j(t) = \left[\frac{V - v_{ox}(t)}{R_{p1} + R_{p2}}\right] \quad (2)$$

where V is the constant voltage applied by the power supply, v_{ox} (t) is the potential difference across the oxide film measured by the voltmeter in Fig. 1, R_{p1} and R_{p2} are the resistances of the potentiometers 1 and 2, respectively. The oxide film growth terminates once the potential difference across the film reaches the applied voltage (constant voltage) and as the current through cell approaches zero in accordance to Eq. (2). The potential difference or anodic voltage rise across the oxide film is measured by a digital voltmeter as a function of time with

reference to the platinum cathode at zero voltage. Therefore, no reference electrode is required. Thus, all *V–I* data are potential rise across the film at constant source voltage. The total charge consumed during the anodization process is measured by a charge integrator. In general, the current flow through the cell at any instant involves the ionic current across the solution between the electrodes, electronic conduction through the metal electrodes and the electron transfer across the metal-solution interface.

The final appearance of the film, however, depends mostly on the cleaning process after the film is made. The following procedure is used: After the film is carefully peeled out from the Lucite flame, it is transferred into a clean solution of trichlor-ethylene and rinsed for about 2 min or until all the grease left from the mounting has been rinsed off. Paint thinner works well for this initial cleaning. The film so rinsed is then flushed with acetone and then with water and air dried. Fast and uniform drying is accomplished by gently blowing nitrogen gas across the film.

Anodizing electrolyte

The electrolytes used are 2.0 mL of natural (non O^{18-} enriched) electrolytic solutions of distilled water of pH 6 with no supporting buffering salt, 3% by weight ammonium citrate solution, water, and biological solutions (urine and blood serum and plasma) of pH ranging from 6.8 to 8.0. These solutions are obtained as described by Nwosu [29]. The normalized enriched water for preparation of the reference standard targets is supplied by Cambridge Isotope Laboratories (CIL). The enriched biological or water solutions used were prepared by diluting known volumes of the standard enriched solutions with known volumes of distilled water. The ammonium citrate solutions were prepared by dissolving 3% by weight of ammonium citrate salt in distilled water and adjusting the pH to 6.0 to 6.4 by adding few drops of NH_4OH.

The ^{18}O enriched serum and plasma samples are prepared by adding one gram of 10 atom% ^{18}O enriched water to each gram of serum and plasma. The final enrichment of the mixture is calculated as 5.1 atom ^{18}O, assuming natural abundance of 0.204 atom% in serum or plasma. Ta_2O_5 targets are then prepared at a voltage of 100 V and 10 mA cm^2 of current density for 10 min.

Basic anodization model

Given the assumption that the concentration of the electrolyte remains relatively constant at the electrolyte interface, and neglecting adsorption and desorption of the reactants, one can assume the dominant mechanism for the anodization process to be driven by electron transfer and diffusion controlled by the potential difference across the electrodes. Thus, within such basic assumption, the present analysis is based on the following four postulates.

1. The total oxide film thickness (Δx) depends on the field strength. Thus, the thickness of the oxide film is proportional to anodic potential difference, Δv_{ox} across the oxide film such that Δx, can be written as:

$$\Delta x = \beta \Delta v_{ox} \tag{3}$$

where β is the anodic constant (the reciprocal of the field strength) that depends on the anode metal-electrolyte interface.

2. Faraday's law is valid. Thus, the rate of increase of the oxide thickness is proportional to the net oxidation current (j_{ox}) and can be expressed as:

$$\frac{dx}{dt} = \chi j_{ox}(t) \tag{4}$$

where $\chi = M/zF\rho A$ depends on the reacting species and gives the film thickness per coulomb of charge transferred, M is the formula weight of Ta_2O_5 (441.8 g mol^{-1}); F is the Faraday's number (96,500 C); z is the number of electrons mol^{-1} which is 10 from Eq. (1); ρ is the density of Ta_2O_5 (8.03 g cm^{-3}); and A is the cross sectional area of the oxide film produced (1.0 cm^2), giving χ as 5.7×10^{-5} (cm C^{-1}), assuming no incorporation of any other oxyanions.

3. Assume continuity conditions on the current is given as:

$$j_t = j_{ox} + j_e + j_s \leq j_0 \tag{5}$$

where j_{ox} is the oxidation current density due to ionic transfer, j_e is the electron current density due to the impact avalanche process and increases with anodic voltage, j_s is the current density due to movement of electrolytic oxyanions at the electrode surface, and j_0 is the initial applied current density. It is hypothesized that the electron current density is governed by:

$$j_e(t) = A(T)\exp(\lambda(T)v_{ox}(t)) \tag{6}$$

where $A(T) = k\, j_{ox}$ is the temperature dependent primary electron current density assumed to be proportional to the oxidation current and $\lambda(T)$ is the temperature dependent ionic transport coefficient that depends on the electrolyte.

4. The electron current density due to movement of oxyanions at the electrode surface is a fraction γ of the oxidation current density so that:

$$j_s = j_{ox}\gamma \tag{7}$$

Substituting Eqs. (6) and (7) into the continuity Eq. (5), the net oxidation current density can be modeled as:

$$j_{ox}(t) = j_t[(1+\gamma) + k\exp(\lambda v_{ox}(t)]^{-1} \tag{8}$$

where k is a constant that depends on the concentration of the oxyanion in the electrolyte.

From Eq. (3), the rate of the oxide growth is directly proportional to the rate of potential rise across the anode such that $dx/dt = \beta dv_{ox}/dt$. Equating this with Eq. (4) and using Eq. (8), we have:

$$\frac{dv_{ox}}{dt}|_{V=\text{constant}} = \left(\frac{\chi j_t}{\beta}\right)[(1+\gamma) + k\exp(\lambda v_{ox}(t)]^{-1} \tag{9}$$

The first and second terms in Eq. (9) are due to net contributions from ionic oxidation and electron currents, respectively. Dividing both sides of Eq. (9) by j_t to express the equation dimensionally as reciprocal of the film capacitance, the film capacitance can be expressed as:

$$C(t) = \frac{\beta}{\chi}[(1+\gamma) + k\exp(\lambda v_{ox}(t))] \tag{10}$$

Results and discussions

Anodization in water

Figures 2 and 3 show variations of electric current density and anodic potential difference (insert) for Ta_2O_5 at

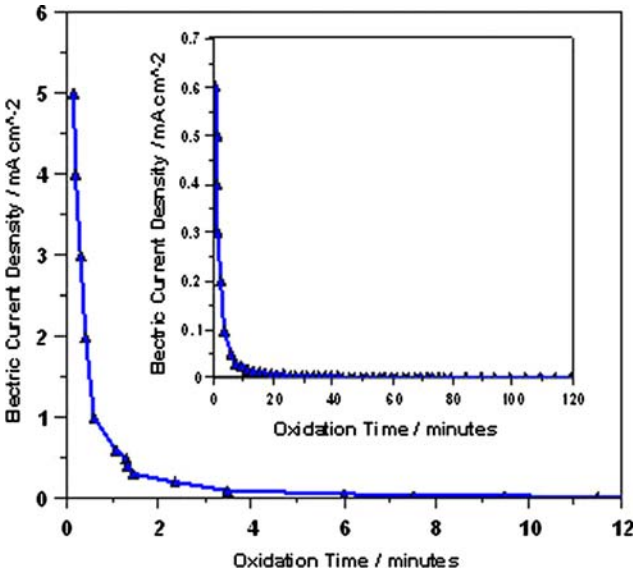

Fig. 2 Variation of electric current density with time

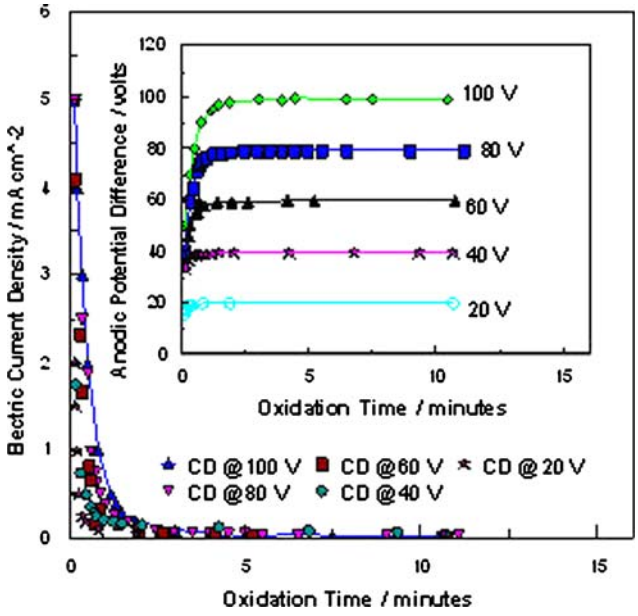

Fig. 3 Variations of electric current density and anodic potential difference (inserted) for 20–100 applied voltage in water (natural)

varying applied voltage distilled water. The insert in Fig. 2 shows the continuous exponential drop in current density as the anodic potential difference approached constant value. The potential difference across the oxide film depends on the total resistance of the oxide film-electrolytic system. During the initial rapid rise in the anodic potential difference, the anodization electric current density falls exponentially due to the continuous increase in field strength, with increasing film thickness. The electric current density is high initially because of the small resistance to current flow. As the oxide increases in thickness, the electrolytic bath-oxide resistance increases. This results in the exponential decrease in electric current density as the potential difference across the film $v_{ox}(t)$ approaches the applied voltage, V and corresponds to the film reaching its maximum capacitance. The rate of oxide growth (current density) becomes so small at this stage that for all practical purposes the thickness, and hence potential difference, may be assumed to have reached a limiting constant value.

Figure 4 shows the alpha particle yield for the anodic films produced in water and biological electrolytes (solid line is reference curve for water). The alpha particle yield is measured by nuclear reaction analysis using 2.0 MeV van der Graaff accelerator [30]. The thickness of the film is directly proportional to the applied voltage, with the proportionality constant given by the inverse of the electric field strength [29]. Note that the lines did not pass through the origin. This is due to the initial thin oxide film layer deposited on the tantalum substrate by spontaneous oxidation.

The comparison of the anodization potential-time curves for polished (solid curve) and unpolished (symbol)

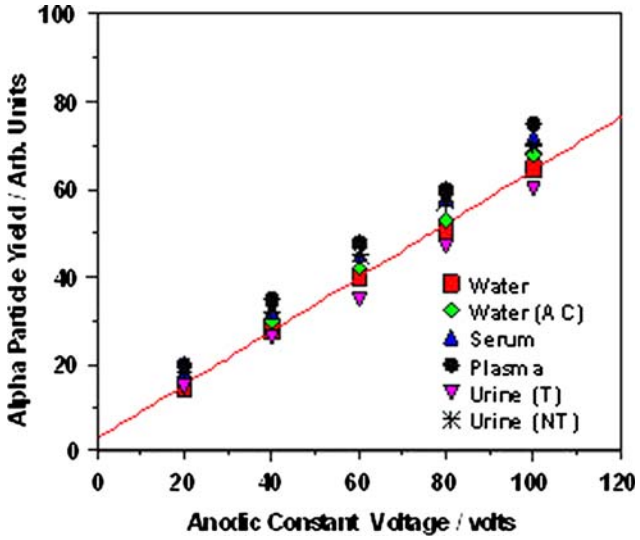

Fig. 4 $^{18}O(p, \alpha)\ ^{15}N$ alpha particle yield as a function of anodic potential from Ta_2O_5 film produced in water, blood serum and plasma treated (T) and non-treated (NT) urine electrolytes

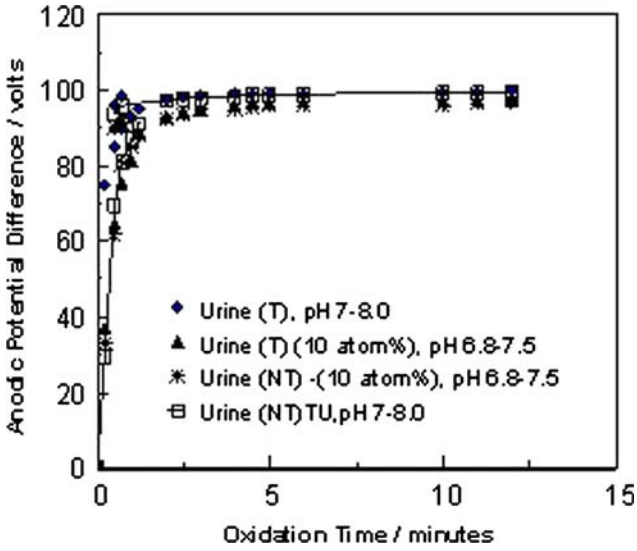

Fig. 6 Anodic potential rise at 10 mA cm^{-2} electric current density for natural treated urine (T), nontreated urine (NT), and 10 atom% ^{18}O enriched treated and non-treated urine electrolytes

tantalum substrates in Fig. 5 shows that there is no significant difference between the anodic mechanism for polished tantalum and the unpolished sample. The results indicate that both polished and unpolished substrates will produce oxide thicknesses that differ by only 3% (16.2 Å V^{-1} in citrate water compared to 15.7 Å V^{-1} in distilled water as shown in Appendix A). However, the use of the polished sample has the added disadvantage of a complex and time consuming preparation techniques.

Anodization in biological solutions

Figure 6 shows a series of anodizations of in treated and untreated urine electrolytes where there the solid curve if for the untreated (natural) urine sample. Similarly, Fig. 7 shows anodizations in water, diluted urine, and blood plasma and serum (solid line is reference curve for water). The objective was to compare individual measurements of Ta_2O_5 targets made in the biological solutions with those of pure water and investigate the effect of reduction of ionic concentration. Anodizations were carried out at 10 mA cm^{-2} electric current density and 100 V applied voltage. The films anodized in treated urine (T) electrolytes were treated with charcoal and filtered with a filter paper to reduce the dissolved impurities while the NT electrolytes

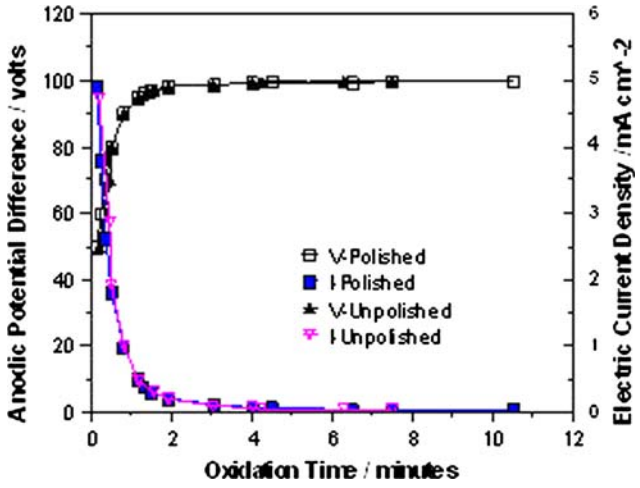

Fig. 5 Anodic potential rise and current drop for polished (solid curve) and unpolished tantalum anodic oxidation in water at 10 mA cm^{-2} electric current density

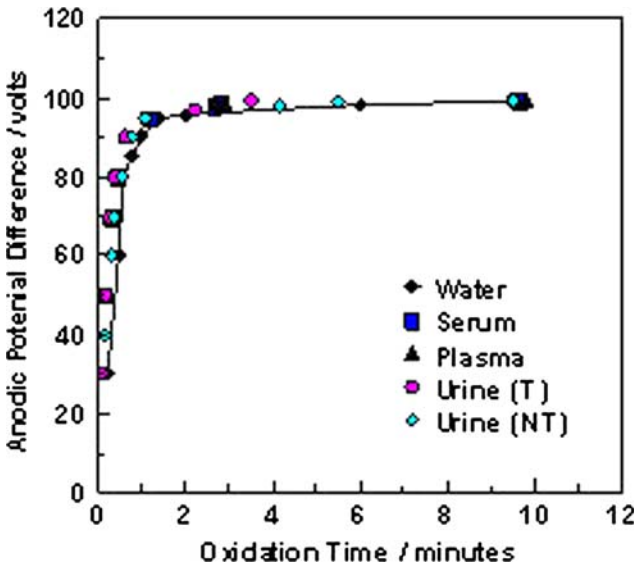

Fig. 7 Anodic potential difference rise at 10 mA cm^{-2} electric current density for water, plasma (PLN), serum (SEN), treated (T) and non-treated (NT) urine samples

were urine samples used in untreated natural state. The enriched electrolytes were prepared by dilutions with known ^{18}O atom% enriched solutions of water. It is clear from the Fig. 6 that the rate of potential rise was higher for the untreated sample than for the treated samples. As shown in Fig. 7, the enrichment of the sample with solutions of enriched water resulted in dilution of the urine sample hence, a reduction in oxidation rate. Similarly, the urine filtration procedure resulted in the reduction of ionic species resulting in reduction in current conduction and therefore oxidation rate.

The plasma and serum electrolytes were not treated in any way. Comparison of these results shows a definite correlation between the potential rise [2, 29] and the electrolytic concentration. The water electrolyte has a pH range of 6.0–6.4 while the biological electrolytes have a pH range of 6.8–8.0 depending on the level of dilution and ionic concentration. The lower anodization rate for the diluted or treated urine sample compared to the untreated plasma and urine sample is due to the fact that the treatment and dilution procedure reduced the ionic concentration, and the pH level to about 6.8–7.5 compared to the untreated sample of pH from 6.5 to 8.0. In general, the oxide growth in biological electrolytes was higher than that in water, with plasma showing slightly higher potential rise than water and other electrolytes tested.

Anodization model

Anodization model expressed by Eqs. (8), (9) and (10) show the dependence of electric current density, oxide film growth, and film capacitance on the potential difference across the film. As shown in Fig. 8, the model (solid line) approximately agrees with the experimental result (symbols) and shows that the rate of oxide growth during the initial stage of the anodic process is higher for the biological solutions than for water. The rate decreases linearly as the film resistance increases or potential difference across the oxide film approaches the applied constant voltage of 100 V after 10 min of oxidation time.

The plot of oxide film capacitance from Eq. (10) in Fig. 9 shows no significant difference in the capacitance-applied potential behavior for water and biological electrolytes. However, a slightly higher asymptotic rise in capacitance is observed for plasma solutions than serum, urine and water closed to the limiting applied potential. The summary of parameters determined for Eq. (9) is shown in Table 1.

It is evident that the biological solutions have a significantly higher ionic transfer coefficient than water. This means that biological medium allows for the transfer of more O^- ions to the anode per a given energy (applied potential). It appears the biological ions act as natural pH

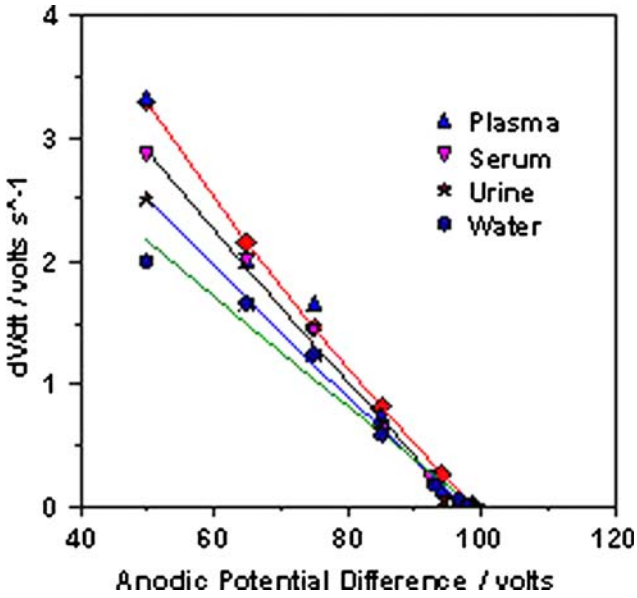

Fig. 8 Variation of rate of oxide growth with anodic potential difference for water and biological solutions at 10 mA cm^{-2} electric current density

buffers resulting in a greater rate of oxide growth for the same applied potential. This also implies that more initial electric current density is available for the growth of the oxide formation in biological samples than in water as evidenced from the $k = j_s/A(T)$ values. Since the *A(T)* value is a definite fraction of the initial oxidation electric current density, the higher *k*-values for the biological solutions implies higher net oxidation current from Eq. (5). Similarly, the γ-values (defined as ratio of electron current to oxidation current) are significantly different and higher

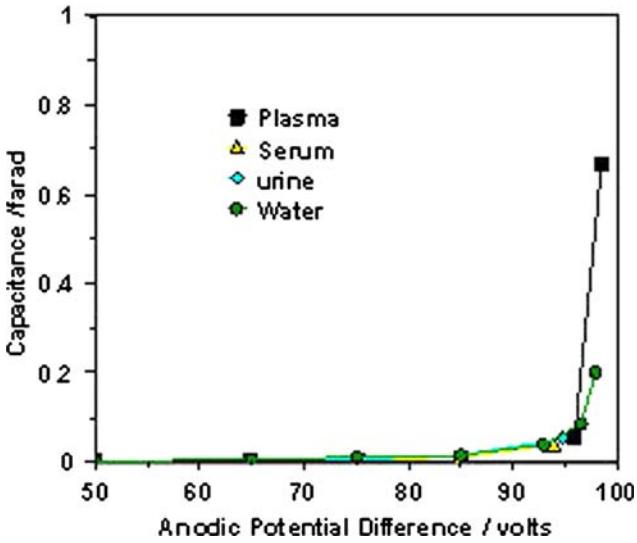

Fig. 9 Variation of oxide film capacitance anodic potential difference for water and biological solutions at 10 mA cm^{-2}

Table 1 Ionic properties (λ, k, and $A(T)$) determined from the non-linear curve fit of Eq. (8) with average $R^2 = 0.99$ temperature $T = 22 \pm 1$ °C

	Plasma	Serum	Urine	Water
pH	7–8.0	7–8.0	7–8.0	6–6.4
λ (V^{-1})	–0.0714	–0.0281	–0.0362	–0.003
$k = j_s/A(T)$	–1.186	–1.489	–1.462	–1.671
A(T)	0.0206	0.0404	0.0271	0.2401
$\gamma = j_e/j_0$	1.402	0.9627	1.0885	0.7218
β (Å/V)	17.5 ± 1.2	17.3 ± 1.2	17.3 ± 0.8	15.7 ± 0.4

in biological solutions than in water. At a high field strength, electrons injected into the oxide conduction band could be accelerated to an energy level that is high enough to free more electrons by an avalanche multiplication. Thus, as the applied potential increases, more electrons are injected into the band. Such an avalanche electron current increases with oxide thickness and has been shown to cause oxide or anodic process breakdown at high fields [28]. The higher γ-values show that oxidation in a biological environment is more likely to break down than in water for the same oxidation time and applied potential. The break down or edge effects can be observed as a series of spikes on the chart recorder as shown in Fig. 10. This observed behavior may be due to the influence of the electron current due to the avalanche process. It appears that the electron current in Eq. (7) is starting to increase greater than the oxidation current (first term). This occurs after 7.5 min oxidation time corresponding to a electric current density of about 0.05 mA cm^{-2}. In more than 90% of the cases, breakdown will not occur below this electric current density.

The aim is to avoid such spikes, especially if they last for more than a few tenths of a second. As indicated in Figs. 2–3, after 7.5 min of oxidation time corresponding to 99.5% of the applied potential, the applied potential difference increases by less than 0.1 V per minute reaching 99% of the applied (constant) potential of 100 V after about 0.5–1 h of oxidation time if the formed oxide does not break down. The breakdown voltage may also be reached if there is a local defect on the metal surface. Thus, because of greater probability of oxide breakdown at high applied potential, the method adopted in the present study is to terminate the process after 10 min or after the electric current density, (monitored by a digital meter), has decreased to 0.04 mA cm^{-2}. It is shown in Fig. 11 that films anodized for 7.5 min are statistically the same as those at 10–60 min. The alpha yield of the film targets produced a limiting applied voltage are statistically the same for current densities from 0.05 mA cm^{-2} to 0.01 mA cm^{-2}.

The film may continue to increase in thickness at longer times due to increased electronic leakage current. The results show that the effect of electron current for a well-prepared surface is negligible for the first 60 min of oxidation.

Figure 12 shows that total oxidation time also influences the extent of the interference coloration. At 80 V applied potential across the anode for oxidation time ranging from 7.5 min to 120 min, the color ranges from light orange to dark red. Figure 13 displays uniform dark blue interference coloration the interference colors for anodization at 100 V applied potential and 12 min of oxidation time. The

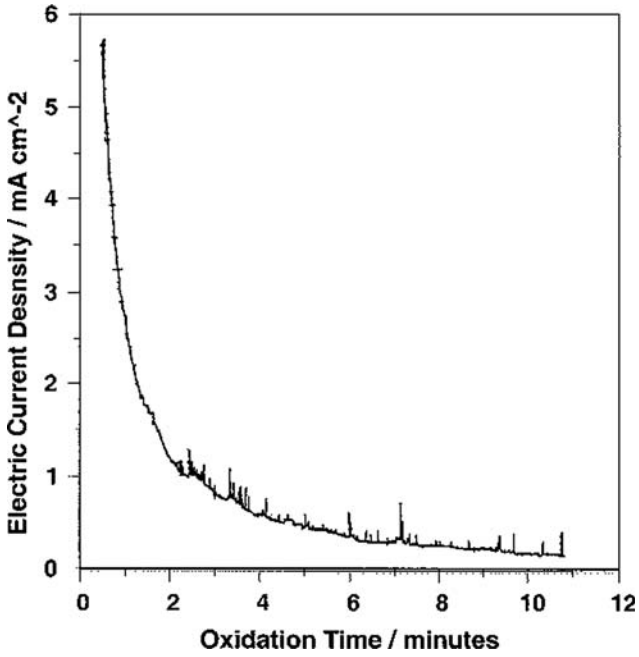

Fig. 10 Fluctuation in electric current density as a function of time during anodic oxide breakdown

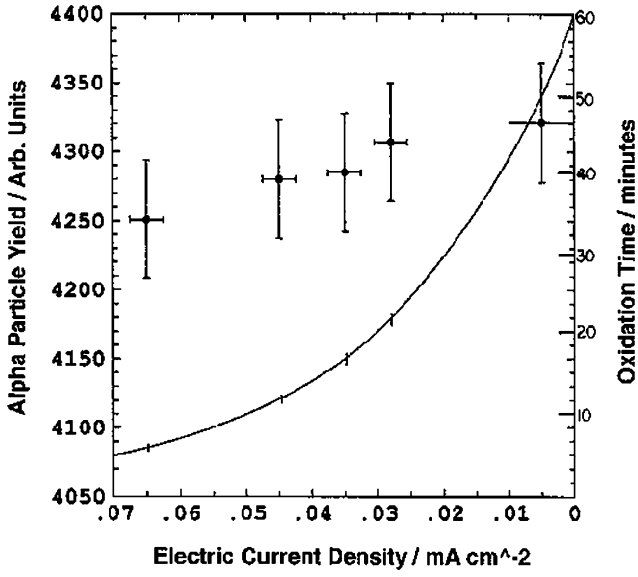

Fig. 11 Variation of alpha particle yield and oxidation time with electric current density

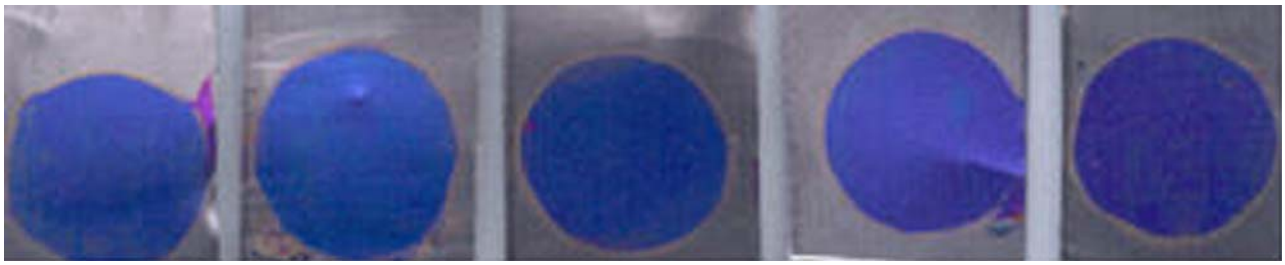

Fig. 12 Anodic Ta_2O_5 film produced at 10 mA cm^{-2} in (**a**) pure water showing light blue to dark blue interference colors at 100 V and orange to violet colors at 80 V and in (**b**) biological solution showing blue to dark blue colors at 100 V and dark orange to dark violet colors in biological solution

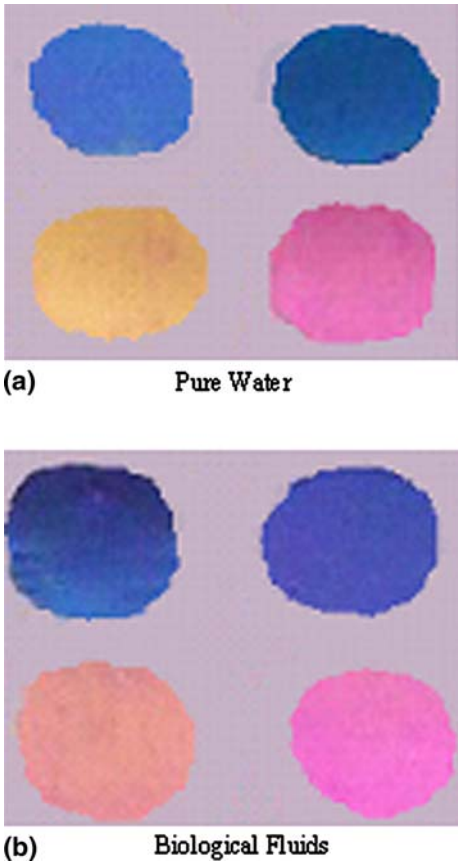

Fig. 13 Anodic Ta_2O_5 film interference (orange to red colors) for 80 V in pure water for 7.5 to 120 min of oxidation time at 10 mA cm^{-2} electric current density

precision and repeatability of anodization method used here is clearly seen.

Figure 14 shows typical interference colors for anodization for applied potential ranging from 80 V to 100 V for pure water and biological (urine) solutions. Comparison of results shows that biological electrolytes on the average produce darker inference colors than in pure water. This is mainly due to higher pH of the biological electrolytes and the higher rate of oxide growth, which results in thicker oxide films in biological electrolyte than in water for the same oxidation time.

Conclusion

A reliable method of preparing Ta_2O film targets in natural water and biological fluids (urine, blood plasma and serum) was developed. Ta_2O_5 film targets are successfully prepared using a electric current density of 10 mA cm^{-2} at anodic potential difference of 100 V without any oxide breakdown. For the same applied potential, more ionic current is available for conduction in biological solutions than in water and the rate of oxide growth during the initial stage of the anodic process is higher for the biological solutions than water. The oxide film capacitance is found to be only slightly dependent on pH and anodic potential difference with higher capacitive films in biological solutions than for water.

Appendix A: Data reduction for determining inverse field strength

The method of determining the electric field strength or the anodic constant is based on the following experimental observations:

1. The thickness of the oxide film (Δx) deposited on the surface of tantalum metal in an electrolyte is proportional to the anodic potential difference across it (voltage, v_{ox}) such that:

$$\Delta x = \beta_e \Delta v_{ox} \tag{A.1}$$

where the constant, β_e is the inverse electric field strength (or anodic constant).

2. The number of ^{18}O atoms, n_{18}, anodically incorporated into the anodized tantalum pentoxide film per unit volume is proportional to ^{18}O content and can be expressed as:

$$n_{18} = N_\rho C[^{18}O]_e \tag{A.2}$$

where $C[^{18}O]_e$ is the atom% or fraction of ^{18}O nuclei in the total amount of oxygen nuclei,

Fig. 14 Anodic Ta_2O_5 film interference (uniform dark blue color) for 100 V in pure water for 12 min of oxidation time at 10 mA cm^{-2} electric current density

$N\rho = 5.5 \times 10^{22}$ atom cm^{-3} is the number density for pure Ta_2O_5 of molecular weight of 442 g mol^{-1} and density of 8.03 g cm^{-3}. For a well defined solid angle and the reaction cross section, the reaction alpha yield rate per unit thickness of the oxide film target is proportional to ^{18}O nuclei deposited on the oxide film from a given electrolyte and given as:

$$\frac{\Delta N_\alpha(e)}{\Delta x} = \lambda C[^{18}O]_e \tag{A.3}$$

where λ in Eq. (A-3) is a lumped experimental factor given as:

$$\lambda = N_\rho Q_p \sigma_\theta(E_p)\Omega \tag{A.4}$$

Ω is the solid angle in steradian subtended by the detector, σ_θ (E_p) is the reaction cross section (in cm^2 sr^{-1} $atom^{-1}$) for the detection angle and proton bombarding energy, E_p, and Q_p is the total number of protons bombarding the target. Substituting Eq. (A.1) into (A.3) gives the alpha yield per oxide potential as:

$$\frac{\Delta N_\alpha(e)}{\Delta v_{ox}} = \beta_e \lambda C[^{18}O]_e \tag{A.5}$$

Solving Eq. (A.5) for β_e gives:

$$\beta_e = k_e\left[\lambda C[^{18}O]_e\right]^{-1} \tag{A.6}$$

where $k_e = \Delta N_\alpha\ (e)/\Delta v_{ox}$ is the slope of the plot of alpha yield versus voltage for Ta_2O_5 films produced in a biological electrolyte.

4. The ^{18}O concentration ratio is the ratio of ^{18}O concentration in the reference electrolyte to ^{18}O concentration in the biological electrolyte of interest and is proportional to the measured alpha particle yield ratio, R_α (e), such that:

$$R_\alpha(e) = \frac{N_\alpha(\text{ref})}{N_\alpha(e)} = R_\beta\left[\frac{C[^{18}O]_{ref}}{C[^{18}O]_e}\right] \tag{A.7}$$

where N_α (ref) and N_α *(e)* are the alpha particle yields from the oxide film made in the reference solution and the biological electrolyte, respectively. The proportionality constant R_β is an important normalization factor that corrects for the difference in inverse electric field strengths of water and biological solution.

Absolute determination of β_e from Eq. (A.6) depends on the precise knowledge of all the lumped experimental factors defined in Eq. (A.4). Fluctuations of the beam current and Q_p value are usually the most difficult to control experimentally. Errors due to the effect of such fluctuations can be minimized if the determination is done relative to the oxide film target prepared in 3% ammonium citrate water or any reference standard solution of choice with known β_{ref} value. Thus, writing Eq. (A.6) for the standard reference solution gives:

$$\beta_{ref} = k_{ref}\left[\lambda C[^{18}O]_{ref}\right]^{-1} \tag{A.8}$$

where k_{ref} is the slope of plot of alpha yield versus voltage for the films produced in the reference solutions. By dividing Eq. (A.6) by (A.8), the inverse electric field strength for the oxide film produced in biological solutions or any solution of interest can be expressed as:

$$\beta_e = \gamma\beta_{ref} \tag{A.9}$$

where

$$\gamma = \left[\frac{C[^{18}O]_{ref}}{C[^{18}O]_e}\right]\left[\frac{k_e}{k_{ref}}\right] \tag{A.10}$$

Equation (A.10) can also be rearranged as:

$$\left[\frac{C[^{18}O]_{ref}}{C[^{18}O]_e}\right] = \gamma\left[\frac{k_{ref}}{k_e}\right] \tag{A.11}$$

Comparing Eq. (A.7) with Eq. (A.11), the proportionality constant $R_\beta = 1/\gamma$ can be determined as the slope of plot of alpha particle yield ratio versus the ^{18}O concen-

tration ratio. When the reference electrolyte has the same ^{18}O concentration as the test biological electrolyte or when both are of natural ^{18}O abundance of 0.204 atom%, the ^{18}O concentration ratio in Eq. (A.10) is unity so that $\gamma = k_e/k_{ref} \sim 1\ R_\alpha\ (e)$ for the same anodic potential difference in both reference and test electrolytes (typically 100 V for these tests).

References

1. Fiegna C, Iwai H, Wada T, Saito M, Sangiorgi E, Ricco B (1994) IEEE Trans Electron Devices ED-41:941
2. Nwosu SN, Fishbeck FJ (1989) Nuclear Inst Method Phys Res B40–B41:833
3. Bradshaw SD, Cohen D, Katsaros A, Tom J, Owen FJ (1987) J Appl Physiol 63(3):1296
4. Resetic A, Jaric B (1990) J Appl Electrochem 20:768
5. Hong YH, Park HD, Jun CB, Lee DD, Kim BR (1992) J Korean Inst Telem Electron 29A:87
6. Hudner J, Hellberg PE, Kusche D, Ohlsen H (1996) Thin Solid Films 281–282:415
7. Roberts S, Ryan J, Nesbit L (1986) J Electrochem Soc 133:1405
8. Nishioka Y, Kimura S, Shinriki H, Mukai K (1987) J Electrochem Soc 134:410
9. Kukli K, Ihanus J, Ritala M, Leskela M (1997) J Electrochem Soc 144:300
10. Zaima S, Furuta T, Yasuida Y, Iida M (1990) J Electrochem Soc 137:1297
11. Ikonopisov S (1977) Electrochim Acta 1077
12. Albella J et al (1980) Appl Electrochem 11:525
13. Young L (1961) Anodic oxide films. Academic Press
14. Amsel G (1972) In: Proceedings of an international colloquium on oxygen isotope. Cadarashe, France, 4–9 Sept
15. Chu WK, Mayer JW, Nicolet MA (1973) Thin Solid Films 17:1
16. Hasegawa, Hartnagel HL (1976) J Electrochem Soc 123:713
17. Delloca CJ, Young LJ (1970) J Electrochem Soc 117:1545
18. Montero I, Pelloie B, Perriere J, Pivin J, Albella JC (1989) J Electrochem Sco 1:1869
19. Montero JM, Albella JM, Martinez-Duart J (1985) Electrochem Soc 132:814
20. Barger FJ, Wu JC (1971) J Electrochem Soc 118:2039
21. Hutchins GA, Chen CT (1986) J Electrochm Soc 133:133
22. Shimizu K, Brown GM, Habazaki H, Kobayashi, Skeldon K, Thompon P, Wood GE (1998) GC Corrosion Science 40(6):963
23. Li YM, Young L (1998) Electrochimica Acta 44(4):605
24. Badawy WA, Ismail KM (1993) Electrochimica Acta 38(15):2231
25. Albella JM, Montero JM, Sanchez O, Martinez-Duart J (1986) J Electrochem Soc 133:876
26. Albella JM, Montero JM, Sanchez O, Martinez-Duart J (1985) Thin Films 125:57
27. Albella JM, Montero JM, Martinez-Duart J (1985) Electrochem Soc 132:976
28. Amsel G, Nadai JP, Ortega C, Rogo S, Seikal J (1978) Nucl Instr Meth 149:705
29. Wosu SN (2005) Nuclear Instrum Methods Phys Res B 237:631
30. Nwosu SN (1988) Ph.D. Dissertation, University Microfilms, Ann Arbor Michigan